Aerosol Scavenging in DC3 and SEAC^{4}RS Deep Convective Storms

Mary C. Barth et al.

Supplementary Text

S1. Description of storm cases included in the analysis

18 May 2012 DC3 case

The 18 May 2012 case, sampled near Ogallala, Nebraska in the vicinity of a cold front, had a SWEAT Index of 283 categorizing it as a moderate, single cell storm. The storm was quite strong with respect to the 20 dBZ cloud top heights of 14 km MSL, reports of hail of one inch diameter (Herndon, 2012a), and periods of high lightning flash rates. The storm had relatively higher anthropogenic and agriculture signatures and lower biogenic signatures based on VOC measurements. The environment had a dry aerosol extinction of 31 Mm^{-1}, which is slightly higher than typical rural conditions (Barth et al., 2015). The BL *f(OA)* was 36%, underscoring the weaker influence of biogenic VOCs.

29 May 2012 DC3 case

The 29 May 2012 storm, sampled north of Oklahoma City, Oklahoma as a line of supercell storms, had a SWEAT Index of 422 producing large hail (up to 3 inch diameter) and a weak tornado. With its high convective available potential energy and 0-6 km wind shear, 20 dBZ cloud top heights exceeded 17 km MSL altitude. Vertical velocities exceeded 50 m s^{-1} (DiGangi et al., 2016). The central Oklahoma region has characteristics of both anthropogenic and biogenic VOCs with nearby oil and gas fields in central Oklahoma and north Texas, urban influences (Oklahoma City), and vegetation in eastern Oklahoma. The BL *f(OA)* was 53% and the dry aerosol extinction was 36 Mm^{-1}, slightly higher than typical rural conditions. This case is the same as that studied by Yang et al. (2015).

02 June 2012 DC3 case

On 2 June 2012, isolated convection was sampled between Greeley and Fort Morgan northeast of Denver, Colorado. The storm can be characterized as moderate convection (SWEAT Index of 256). While storm reports do not include observations of hail, there were reports of surface winds > 33 m s^{-1} (Herndon, 2012b). The 20 dBZ cloud top heights reached 15 km MSL. Like the 18 May case, the chemical environment showed signatures of anthropogenic influences from the Front Range of Colorado and smaller biogenic VOC mixing ratios. The dry aerosol extinction was low (12 Mm^{-1}) and the BL *f(OA)* was 58%.

06 June 2012 DC3 case

Convection on 6 June 2012 was associated with the "Denver cyclone," where low-level flow is southeasterly on the plains east of Denver and is northwesterly to the west of Denver, Colorado. The strong convection occurred just northeast of Denver and had a SWEAT Index of 296, 20 dBZ cloud top heights of 15 km MSL, and storm reports of one-inch diameter hail (Herndon, 2012b). Both the biogenic and anthropogenic VOC mixing ratios in the BL were low relative to other Colorado cases. The dry aerosol extinction was typical of rural background conditions (24 Mm^{-1}) and the BL *f(OA)* was 50%.

16 June 2012 DC3 case

Multicell convection occurred on 16 June 2012 in central Oklahoma. Its SWEAT Index of 360 categorized it as a severe storm. The 20 dBZ cloud top heights reached 15 km MSL. In contrast to the 29 May storm in Oklahoma, both the anthropogenic and biogenic signatures of VOCs were low in the vicinity of this storm. The dry aerosol extinction was low (20 Mm^{-1}), typical of rural conditions. The BL *f(OA)* was 45%.

22 June 2012 DC3 case

The 22 June 2012 case had two severe convective storms occur along the Colorado-Nebraska border (at 41°N). The north storm was unique in that it ingested a wildfire smoke plume at 7 km MSL elevation, while the south storm did not ingest this smoke plume (Barth et al., 2015; Apel et al., 2015). The scavenging efficiency is estimated for only the south storm. The SWEAT Index for these storms was very high (442), cloud top heights reached 18 km MSL and there were reports of 1–2-inch hail for both storms (Herndon, 2012b). The smoke plume came from the High Park Fire west of Fort Collins, Colorado which had been burning for ~2 weeks. Biomass burning was occurring throughout the Rocky Mountain region resulting in its higher contribution to the atmospheric composition in the troposphere. The dry aerosol extinction was high (41 Mm^{-1}) for the region and BL *f(OA)* was 59%. Like other northeast Colorado storms, the biogenic VOCs were low relative to the anthropogenic VOCs (Barth et al., 2015).

02 September 2013 SEAC^{4}RS case

On 2 September 2013 a frontal system extending from north of the Great Lakes to southwest Texas was moving eastward across the US (Cuchiara et al., 2020). Associated with this front was the development of pre-frontal convection in Mississippi mostly of the form of airmass and multicell storms. The SWEAT Index calculated from the 1200 UTC Jackson, Mississippi NWS sounding was 214, while the SWEAT Index calculated from aircraft observations near the two storms was 225 for the airmass storm and 209 for the multicell storm (Table 1). In general, these storms were weaker than the storms sampled in Colorado and Oklahoma during DC3. The airmass and multicell storm cloud top heights were 8 km MSL and 13 km MSL, respectively, and the maximum radar reflectivity was lower in the airmass storm (45 dBZ) compared to the multicell storm (55 dBZ). The pre-frontal convection occurred mid-day (1800-1900 UTC; 1300-1400 LT) in a region rich in biogenic VOCs and low in anthropogenic VOCs (average BL mixing ratios were 1200 pptv isoprene and 39 pptv toluene). The dry aerosol extinction was high (47 Mm^{-1}) for the region with BL *f(OA)* of 54%.

18 September 2013 SEAC^{4}RS case

On 18 September 2013, the position of the "Bermuda High" pressure system over the mid-Atlantic coast and two low pressure systems over the Yucatan Peninsula and west coast of Mexico favored southeasterly flow from the Gulf of Mexico toward southern Texas giving moderate instability off the Texas coast and inland (Cuchiara et al., 2023). As a result, convection occurred over the Gulf of Mexico near Corpus Christi, Texas as well as to the south of San Antonio, Texas. The convection was sampled in the late morning to midday (16:00 – 19:00 UTC, 11:00 – 14:00 LT). To calculate the SWEAT Index, we used aircraft vertical profiles near the convection since the NWS Corpus Christi radiosonde occurred at least four hours before the convection was sampled. The SWEAT Index indicated weak to moderate convection for both the marine (SWEAT = 242) and land (SWEAT = 257) convection. The 20 dBZ cloud

top heights for both marine and land convection reached 8 km MSL and the maximum radar reflectivities were 45-50 dBZ. Being in the same southeasterly flow, the chemical environment was clean for both marine and land convection. Average BL mixing ratios for isoprene and toluene were <60 pptv and the aerosol dry extinction was <12 Mm^{-1} over both the marine and land regions. This contrasts with the findings by Cuchiara et al. (2023) who reported differences in cloud condensation nuclei (CCN) concentrations (282 cm^{-3} and 484 cm^{-3} in the marine and land convective inflow regions, respectively) and cloud characteristics of LWC, cloud base height, and updraft velocity. The BL *f(OA)* was 22% and 34% for the marine and land regions, respectively, which is smaller than the other cases analyzed in this study.

Supplementary Figures

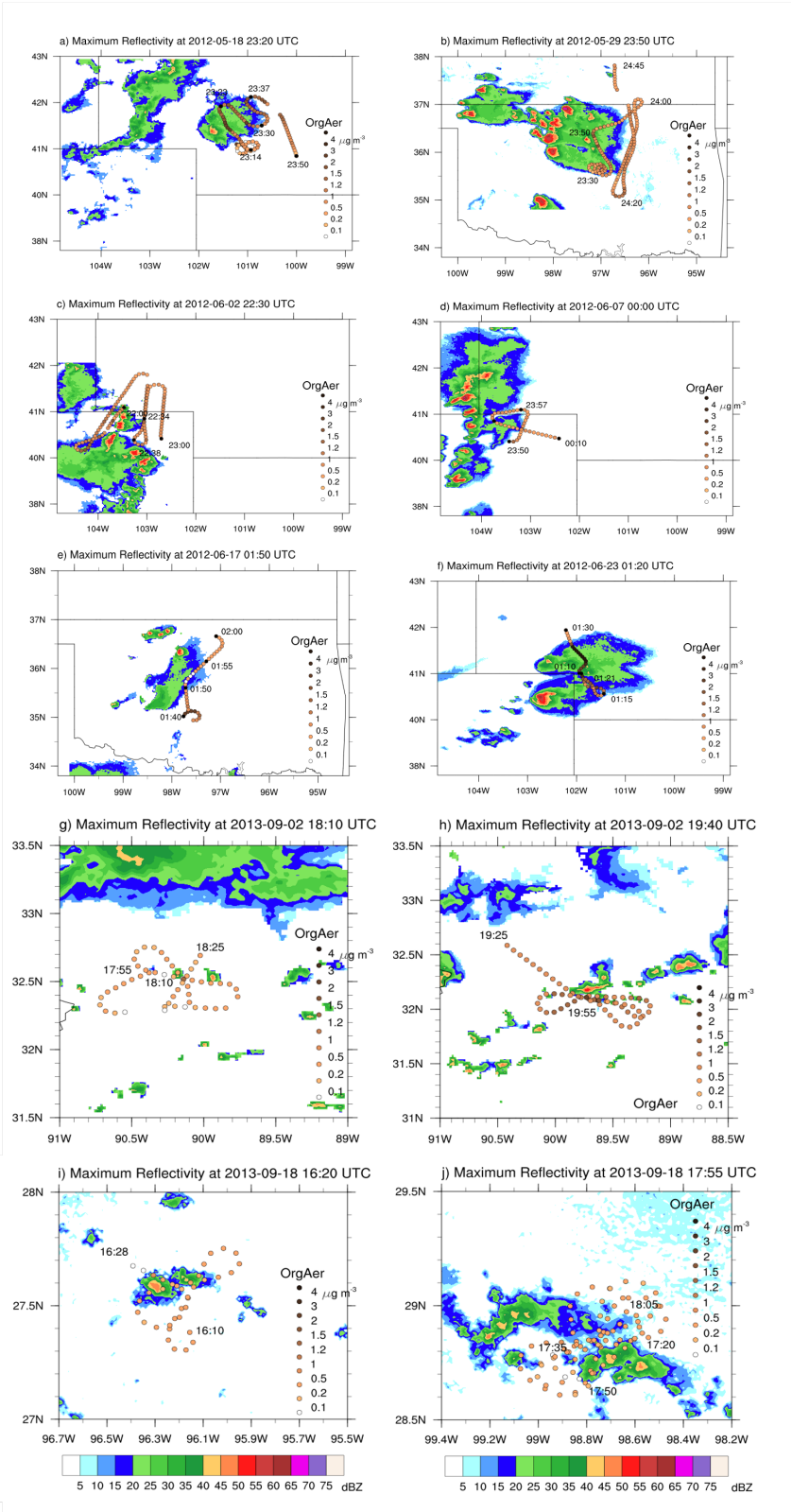

Figure S1. Maximum radar reflectivity in each vertical column for the ten cases analyzed, a) 18 May 2012, b) 29 May 2012, c), 2 June 2012, d) 6 June 2012, e) 16 June 2012, f) 22 June 2012, g) 2 September 2013 air mass storm, h) 2 September 2013 multicell storm, i) 18 September 2013 Gulf of Mexico storm, and j) 18 September 2013 South Texas storm. Overlaid is the DC-8 flight track in the storm outflow colored by the organic aerosol mass concentration (μg std m^{-3}).

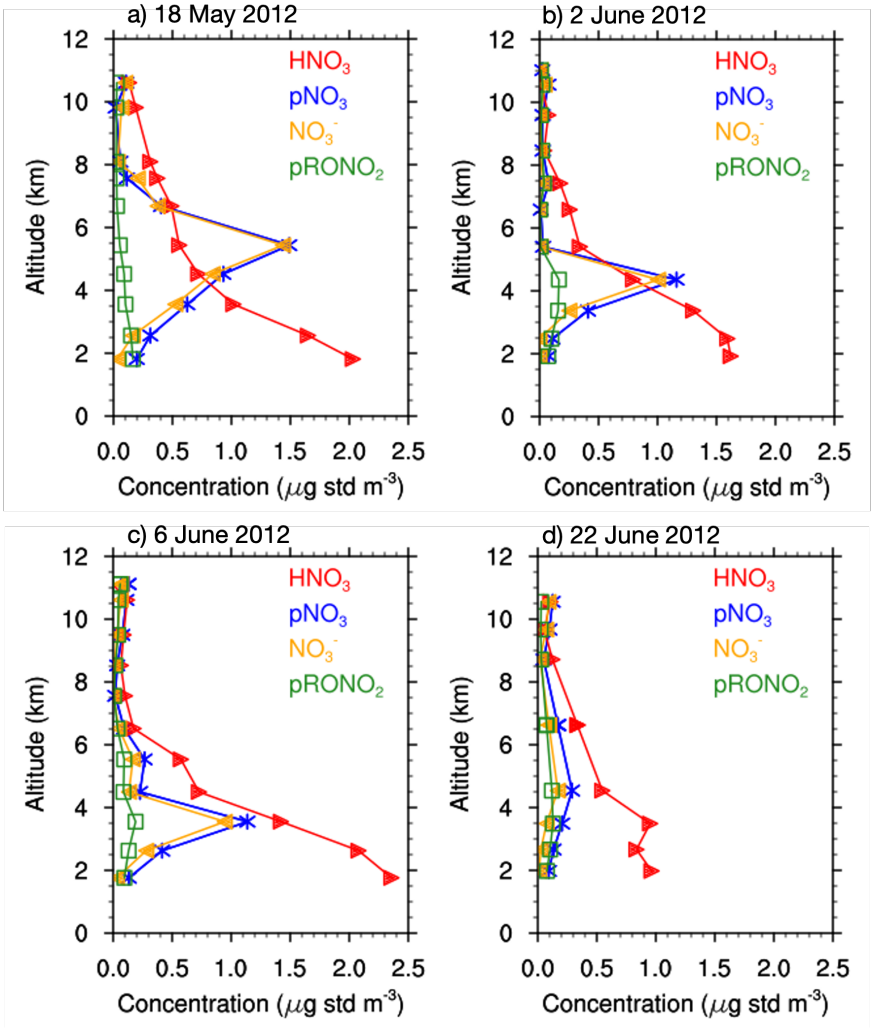

Figure S2. Clear air vertical profiles of HNO_3 (red), particulate nitrate (blue), inorganic particulate nitrate (gold), and organic particulate nitrate (green) for a) 18 May, b) 2 June, c) 6 June, and d) 22 June DC3 storms.

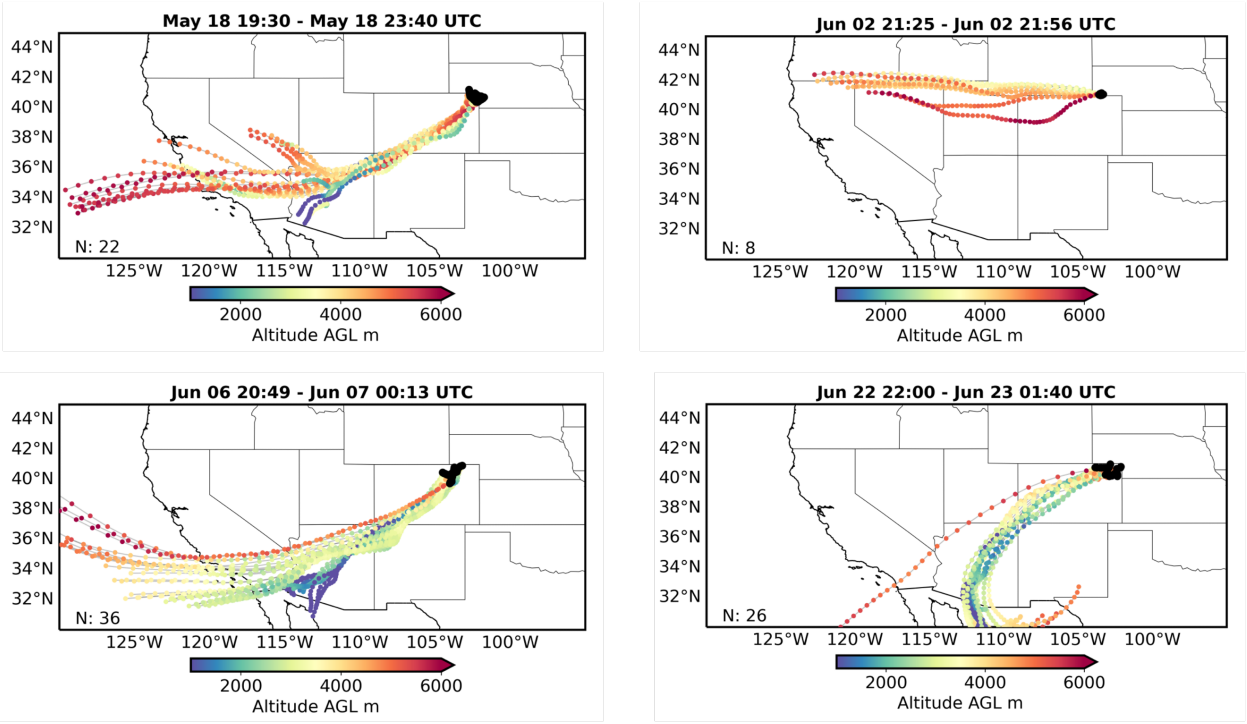

Figure S3. HYSPLIT 48-hour back trajectories calculated for four DC3 storms.

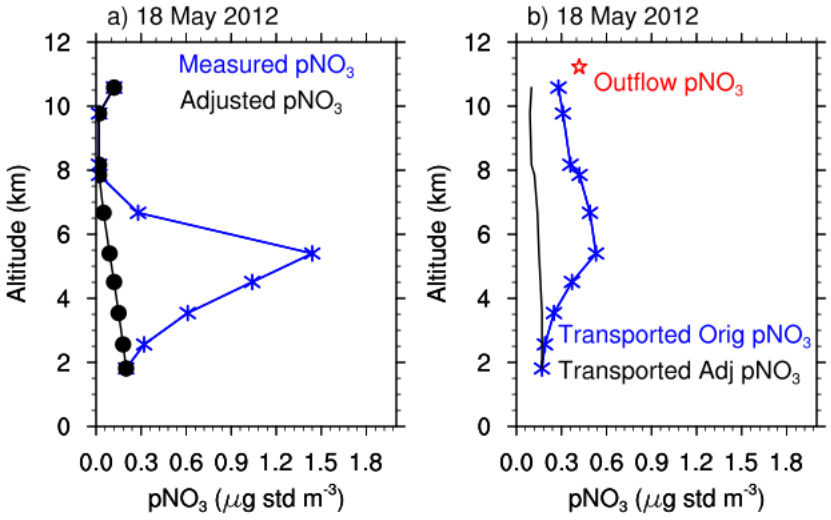

Figure S4. Vertical profiles of particulate nitrate (left) that were measured (blue) and adjusted to remove the mid-troposphere layer (black) and of transported particulate nitrate calculated by the entrainment model (right) with calculated values using the measured clear sky vertical profile (blue) and those using the adjusted clear sky vertical profile (black) for the 18 May 2012 case. The red circle marks the measured concentration of the outflow particulate nitrate concentration.

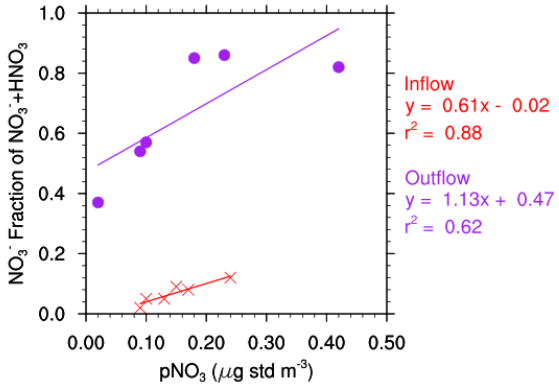

Figure S5. Scatter plot of pNO3 and the NO_3^- fraction of NO_3^- + HNO_3 for the six DC3 cases. Purple solid circles are for the convective outflow regions and red crosses are for the inflow regions.

Supplementary Tables

Table S1. List of data and instruments used in the analysis.

Species/Parameter	Instrument[a]	Uncertainty	Reference
SO_4^{2-}, NH_4^+, NO_3^-, OA, *m*/z 44 for submicron aerosol mass	CU aircraft AMS	Inorganics 34%, Organics 38% (2 sigma)	DeCarlo et al. (2006), Guo et al. (2021)
CO	DACOM	5% or 1 ppmv	Sachse et al. (1987)
CO_2	AVOCET	0.25 ppmv	Vay et al. (2011)
n-butane, i-butane, n-pentane, i-pentane, isoprene, toluene	WAS	5% or 3 pptv	Simpson et al. (2011)
isoprene, toluene	PTR-MS	5%	de Gouw and Warneke (2007)
Aerosol dry extinction at 532 nm	NASA/LaRC optical aerosol measurements	5%	Wagner et al. (2015)
BC	HD-SP2	30%	Schwarz et al. (2013)
HCN	CIT-CIMS	50% + 50 pptv	Crounse et al. (2006)
CH_3CN	PTR-MS	25 pptv	de Gouw and Warneke (2007)
MPN, ANs, PNs	TD-LIF	MPN, ANs: 15% PNs: 10%	Nault et al. (2015)
HNO_3	CIT-CIMS	30% + 50 pptv	Crounse et al. (2006)
O_3	CSD CL	0.040 ppbv + 3%	Ryerson et al. (2000); Pollack et al. (2011)
OH	ATHOS	32%	Faloona et al. (2004)
Aerosol number	SMPS	10%	Wang and Flagan (1993)
Pressure, Temperature, 3D Winds	MMS	Pressure: 0.5% Temperature: 0.2% Winds: 3%	Chan et al. (1998)
Ice water content	2D-S	Not available	Lawson et al. (2011)

[a]CU-HR-TOF-AMS is the University of Colorado High Resolution, Time of Flight, Aerosol Mass Spectrometer; DACOM is the Differential Absorption CO Measurement; AVOCET is the Atmospheric Vertical Observation of CO2 in the Earth's Troposphere; WAS is the Whole Air Sampler that uses gas chromatography; PTR-MS is the Institut fuer Ionenphysik und Angewandte Physik Proton Transfer Mass Spectrometer; HD-SP2 is the Humidified Dual Single Particle Soot Photometer; CIT-CIMS is California Institute of Technology chemical ionization mass spectrometry; TD-LIF is thermal dissociation – laser induced fluorescence; CSD CL is NOAA Chemical Science Division chemiluminescence; ATHOS is the Airborne Tropospheric Hydrogen Oxides Sensor; SMPS is the Scanning Mobility Particle Sizer; MMS is Meteorological Measurement System; 2D-S is two-dimensional stereo probe.

Table S2. NASA DC-8 aircraft inflow and outflow times, their associated altitudes, and entrainment rates for each storm analyzed.

Campaign and Date (mm/dd/yy)	Inflow Altitude (km)	Inflow Time (UTC)	Outflow Altitude (km)	Outflow Time (UTC)	Entrain. Rate (% km^{-1})
DC3 05/18/12	1.7	22:48:29-22:51:10	11.3	23:17:50-23:22:00	14.7
DC3 05/29/12	1.3	23:10:21-23:15:53	11.0	23:48:30-23:58:13	7.8
DC3 06/02/12	1.9	21:16:18-21:27:38	11.1	22:34:14-22:46:10	11.5
DC3 06/06/12	1.7	22:13:40-22:25:12	12.4	23:56:00-24:10:00	4.1
DC3 06/16/12	0.95	24:15:00-24:20:00	11.9	25:50:00-25:55:00	15.4
DC3 06/22/12	2.0	22:31:27-22:45:54	11.2	25:13:52-25:14:38 25:16:51-25:19:24	4.1
SEAC^{4}RS 09/02/13 Airmass	0.8	16:53:11-16:53:551	8.0 8.0 8.0	18:09:45-18:10:15 18:16:03-18:16:32 18:23:16-18:23:33	33.3 11.3 18.2
SEAC^{4}RS 09/02/13 Multicell	0.4	22:12:01-22:18:14	12.0 12.0	19:31:10-19:31:55 19:53:34-19:54:11	10.2 12.5
SEAC^{4}RS 09/18/13 Marine	0.6	15:38:35-15:39:18	8.1 8.1 8.1	16:15:13-16:15:16 16:20:34-16:20:36 16:21:01-16:21:10	9.6
SEAC^{4}RS 09/18/13 Land	0.9	18:30:58-18:35:38	10.1 10.2 10.7 11.3 12.0 12.0 11.1	17:16:40-17:16:47 17:17:01-17:17:19 17:22:23-17:22:30 17:27:48-17:27:58 17:35:31-17:35:40 17:40:28-17:40:41 17:46:39-17:46:48	7.8

Table S3. Inflow, outflow, and calculated aerosol concentrations (μg std m^{-3}) for each case and the estimated scavenging efficiency (%) given as averages ± standard deviation.

Date	Measured Inflow Concentration[a]	Measured Outflow Concentration[a]	Calculated Cloud Top Concentration[b]	Scavenging Efficiency[b,c,d]
		Sulfate		
18 May 2012	2.93 ± 0.16	0.44 ± 0.14	1.19	63.5
29 May 2012	2.11 ± 0.24	0.16 ± 0.07	1.19	86.8
02 June 2012	0.80 ± 0.09	0.18 ± 0.08	0.42	56.7
06 June 2012	2.00 ± 0.26	0.15 ± 0.07	1.49	89.7
16 June 2012	1.58 ± 0.16	0.06 ± 0.05	0.67	90.7
22 June 2012	1.33 ± 0.16	0.26 ± 0.02	1.13	77.3 ± 1.5
02 Sept 2013[e]	3.45 ± 0.27	0.10 ± 0.04	0.93	88.9
02 Sept 2013	3.22 ± 0.46	0.12 ± 0.04	1.20 ± 0.17	90.3 ± 1.6
18 Sept 2013[e]	1.71 ± 0.37	*0.11 ± 0.06*	0.89	100
18 Sept 2013	1.48 ± 0.45	0.08 ± 0.02	0.75 ± 0.03	89.8 ± 3.1
		Ammonium		
18 May 2012	1.15 ± 0.07	0.31 ± 0.09	0.51	39.2
29 May 2012	0.87 ± 0.09	0.09 ± 0.03	0.48	81.2
02 June 2012	0.33 ± 0.04	0.12 ± 0.05	0.18	37.0
06 June 2012	0.72 ± 0.09	0.08 ± 0.02	0.55	86.0
16 June 2012	0.58 ± 0.05	0.03 ± 0.02	0.24	87.6
22 June 2012	0.50 ± 0.05	0.15 ± 0.01	0.46	66.9 ± 1.8
02 Sept 2013[e]	0.95 ± 0.07	*0.02 ± 0.02*	0.22	100
02 Sept 2013	0.83 ± 0.14	0.07 ± 0.04	0.30 ± 0.04	75.0 ± 15.8
18 Sept 2013[e]	0.10 ± 0.03	*0.001 ± 0.001*	0.05	100
18 Sept 2013	0.40 ± 0.10	*0.001 ± 0.001*	0.18 ± 0.01	100
		Nitrate		
18 May 2012	0.17 ± 0.05	0.42 ± 0.12	0.28	–
29 May 2012	0.24 ± 0.04	0.09 ± 0.05	0.15	39.6
02 June 2012	0.10 ± 0.02	0.18 ± 0.08	0.13	–
06 June 2012	0.13 ± 0.03	0.10 ± 0.05	0.16	40.8
16 June 2012	0.15 ± 0.03	*0.02 ± 0.04*	0.13	82.8
22 June 2012	0.09 ± 0.03	0.23 ± 0.02	0.18	–
02 Sept 2013[e]	0.18 ± 0.04	0.08 ± 0.14	0.05	–
02 Sept 2013	0.07 ± 0.03	0.33 ± 0.03	0.09 ± 0.00	–
18 Sept 2013[e]	*0.03 ± 0.01*	*0.01 ± 0.01*	0.02	NaN
18 Sept 2013	0.08 ± 0.07	*0.03 ± 0.01*	0.04 ± 0.00	100
		Organic Aerosol		
18 May 2012	6.05 ± 0.42	1.92 ± 1.06	2.53	24.3
29 May 2012	8.76 ± 0.71	0.74 ± 0.51	4.55	83.8
02 June 2012	3.48 ± 0.40	0.90 ± 0.59	1.68	46.4
06 June 2012	4.89 ± 0.38	0.51 ± 0.31	3.70	86.3
16 June 2012	4.12 ± 0.54	0.19 ± 0.39	1.80	89.5
22 June 2012	5.80 ± 0.39	1.64 ± 0.52	5.19	68.4 ± 10.0
02 Sept 2013[e]	5.92 ± 0.46	0.86 ± 1.97	1.68	49.0
02 Sept 2013	6.46 ± 1.51	1.49 ± 0.88	2.50 ± 0.32	42.3 ± 27.9
18 Sept 2013[e]	0.66 ± 0.18	*0.31 ± 0.16*	0.42	100
18 Sept 2013	1.05 ± 0.33	*0.28 ± 0.13*	0.54 ± 0.01	100

[a]Average concentrations below the detection limit are shown in italics.

[b]For cases where the outflow leg is below the detection limit, the scavenging efficiency is shown as 100% since the measured outflow concentration is not statistically different than zero.

[c]For cases with one outflow leg (Table S2), there is no scavenging efficiency standard deviation calculated.

[d]For cases marked with a dash, the scavenging efficiency is not given because the outflow concentration is greater than the inflow concentration. The case marked NaN is not a number because both the inflow and outflow measured concentrations are below the detection limit.

[e]Measurements from the outflow intercepts were combined to have a larger sample size for the scavenging efficiency calculation.

Table S4. Inorganic nitrate partitioning ratios: $NO_3^-/(NO_3^-+HNO_3)$.

Date	Inflow	Outflow
18 May 2012	0.08	0.82
29 May 2012	0.12	0.54
02 June 2012	0.05	0.85
06 June 2012	0.05	0.57
16 June 2012	0.09	0.37
22 June 2012	0.02	0.86

Table S5. Inflow and outflow particulate inorganic nitrate (NO_3^-), and particulate organic nitrate ($pRONO_2$) average ± standard deviation concentrations (μg std m^{-3}) and their estimated scavenging efficiency (%) for the DC3 cases.

Date	Measured Inflow Concentration[a]	Measured Outflow Concentration[a]	Scavenging Efficiency[b]
	NO_3^-		
18 May 2012	0.02 ± 0.02	0.31 ± 0.14	–
29 May 2012	0.07 ± 0.01	0.03 ± 0.01	42.6
02 June 2012	*0.00 ± 0.00*	0.11 ± 0.01	–
06 June 2012	0.03 ± 0.01	0.04 ± 0.02	39.8
16 June 2012	*0.00 ± 0.00*	–	–
22 June 2012	0.01 ± 0.01	0.15 ± 0.01	–
	$pRONO_2$		
18 May 2012	0.16 ± 0.02	0.13 ± 0.08	–
29 May 2012	0.16 ± 0.03	0.05 ± 0.03	56.9
02 June 2012	0.09 ± 0.01	0.07 ± 0.03	10.5
06 June 2012	0.09 ± 0.01	0.05 ± 0.02	35.7
16 June 2012	0.15 ± 0.02	–	–
22 June 2012	0.08 ± 0.01	0.06 ± 0.01	17.2[c]

[a]Concentrations where total particulate nitrate (pNO_3) was greater than the detection limit but apportioned NO_3^- or $pRONO_2$ was below the detection limit are shown in italics. An apportionment is not possible when pNO_3 is below the detection limit (Day et al., 2022); these cases are marked as missing values.

[b]Unreported scavenging efficiencies are due to outflow concentrations being greater than inflow concentrations or the calculated cloud top concentration is less than the outflow concentration (18 May 2012 case for $pRONO_2$).

[c]Uncertain result as the clear-sky concentrations contained missing data in the mid-troposphere that was filled with the average clear sky concentration between two altitudes.

References

Chan, K. R., Dean-Day, J., Bowen, S. W., and Bui, T. P.: Turbulence measurements by the DC-8 meteorological measurement system. Geophys.Res. Lett., 25(9), 1355–1358. doi:10.1029/97GL03590, 1998.

Crounse, J. D., McKinney, K. A., Kwan, A. J., and Wennberg, P. O.: Measurement of gas-phase hydroperoxides by chemical ionization mass spectrometry. Analytical Chemistry, 78(19), 6726–6732. doi:10.1021/ac0604235, 2006.

Day, D. A., Campuzano-Jost, P., Nault, B. A., Palm, B. B., Hu, W., Guo, H., Wooldridge, P. J., Cohen, R. C., Docherty, K. S., Huffman, J. A., de Sá, S. S., Martin, S. T., and Jimenez, J. L.: A systematic re-evaluation of methods for quantification of bulk particle-phase organic nitrates using real-time aerosol mass spectrometry, Atmos. Meas. Tech., 15, 459–483, doi:10.5194/amt-15-459-2022, 2022.

DeCarlo, P., Kimmel, J., Trimborn, A., Northway, M., Jayne, J., Aiken, A., Gonin, M., Fuhrer, K., Horvath, T., Docherty, K., Worsnop, D., and Jimenez, J.: Field-deployable, high-resolution, time-of-flight aerosol mass spectrometer, Anal. Chem., 78, 8281–8289, doi:10.1021/ac061249n, 2006.

de Gouw, J. and Warneke, C:, Measurements of volatile organic compounds in the Earth's atmosphere using proton-transfer-reaction mass spectrometry, Mass Spectrom. Rev., 26, 223–257, doi:10.1002/mas.20119, 2007.

Faloona, I. C., Tan, D., Lesher, R. L., Hazen, N. L., Frame, C. L., Simpas, J. B., Harder, H., Martinez, M., Di Carlo, P., Ren, X. R., and Brune, W. H.: A laser-induced fluorescence instrument for detecting tropospheric OH and HO2: Characteristics and calibration, J. Atmos. Chem., 47, 139–167, doi:10.1023/B:JOCH.0000021036.53185.0e, 2004.

Guo, H., Campuzano-Jost, P., Nault, B. A., Day, D. A., Schroder, J. C., Kim, D., Dibb, J. E., Dollner, M., Weinzierl, B., Jimenez, J. L.: The importance of size ranges in aerosol instrument intercomparisons: a case study for the Atmospheric Tomography Mission, Atmos. Meas. Tech. 14, 3631–3655, doi:10.5194/amt-14-3631-2021, 2021.

Lawson, R. P.: Effects of ice particles shattering on the 2D-S probe. Atmospheric Measurement Techniques, 4(7), 1361–1381. doi:10.5194/amt-4-1361-2011, 2011.

Nault, B. A., Garland, C., Pusede, S. E., Wooldridge, P. J., Ullmann, K., Hall, S. R., and Cohen, R. C.: Measurements of $CH_3O_2NO_2$ in the upper troposphere, Atmos. Meas. Tech., 8, 987–997, doi:10.5194/amt-8-987-2015, 2015.

Pollack, I. B., Lerner, B. M., and Ryerson, T. B.: Evaluation of ultraviolet light-emitting diodes for detection of atmospheric NO_2 by photolysis - chemiluminescence, J. Atmos. Chem., 65, 111–125, doi:10.1007/s10874-011-9184-3, 2011.

Ryerson, T. B., Williams, E. J., and Fehsenfeld, F. C.: An efficient photolysis system for fast-response NO2 measurements, J. Geophys. Res., 105(D21), 26447–26461, doi:10.1029/2000JD900389, 2000.

Sachse, G. W., Hill, G. F., Wade, L. O., and Perry, M. G.: Fast-response, high-precision carbon monoxide sensor using a tunable diode laser absorption technique. J. Geophys. Res., 92(D2), 2071–2081. doi:10.1029/JD092iD02p02071, 1987.

Schwarz, J. P., Samset, B. H., Perring, A. E., Spackman, J. R., Gao, R. S., Stier, P., Schulz, M., Moore, F. L., Ray, E. A., and Fahey, D. W.: Global-scale seasonally resolved black carbon vertical profiles over the Pacific, Geophys. Res. Lett., 40, 5542–5547, doi:10.1002/2013GL057775, 2013.

Simpson, I. J., Akagi, S. K., Barletta, B., Blake, N. J., Choi, Y., Diskin, G. S., Fried, A., Fuelberg, H. E., Meinardi, S., Rowland, F. S., Vay, S. A., Weinheimer, A. J., Wennberg, P. O., Wiebring, P., Wisthaler, A., Yang, M., Yokelson, R. J., and Blake, D. R.: Boreal forest fire emissions in fresh Canadian smoke plumes: C1-C10 volatile organic compounds (VOCs), CO_2, CO, NO_2, NO, HCN and CH_3CN, Atmos. Chem. Phys., 11, 6445–6463, doi:10.5194/acp-11-6445-2011, 2011.

Vay, S. A., Choi, Y., Vadrevu, K. P., Blake, D. R., Tyler, S. C., Wisthaler, A., Hecobian, A., Kondo, Y., Diskin, G. S., Sachse, G. W., Woo, J.-H., Weinheimer, A. J., Burkhart, J. F., Stohl, A., and Wennberg, P. O.: Patterns of CO_2 and radiocarbon across high northern latitudes during IPY 2008, J. Geophys. Res. 116, D14301, doi:10.1029/2011JD015643, 2011.

Wagner, N. L., Brock, C. A., Angevine, W. M., Beyersdorf, A., Campuzano-Jost, P., Day, D., de Gouw, J. A., Diskin, G. S., Gordon, T. D., Graus, M. G., Holloway, J. S., Huey, G., Jimenez, J. L., Lack, D. A., Liao, J., Liu, X., Markovic, M. Z., Middlebrook, A. M., Mikoviny, T., Peischl, J., Perring, A. E., Richardson, M. S., Ryerson, T. B., Schwarz, J. P., Warneke, C., Welti, A., Wisthaler, A., Ziemba, L. D., and Murphy, D. M.: In situ vertical profiles of aerosol extinction, mass, and composition over the southeast United States during SENEX and SEAC^{4}RS: observations of a modest aerosol enhancement aloft, Atmos. Chem. Phys., 15, 7085–7102, doi:10.5194/acp-15-7085-2015, 2015.

Wang S. C. and Flagan, R. C.: Scanning Electrical Mobility Spectrometer. Aerosol Sci. Technol. 13, 230–240, doi: 10.1080/02786829008959441, 1990.